ISSN: 2755-0168

Journal of Biotechnology & Bioinformatics Research

SCIENTIFIC Research and Community

Review Article

Open Access

Post-Impact Hardness Characterization and Strain Hardening Behavior of Astm A36 Steel Subjected to High-Speed Impact Loading

Muna Slewa[1]* and Pratik Sarker[2]

Department of Mechanical Engineering, Embry-Riddle Aeronautical University, Prescott, Arizona, USA

ABSTRACT

ASTM A36 steel is widely used in structural and industrial applications due to its favorable combination of strength, ductility, weldability, machinability, and low cost. Understanding the behavior of A36 steel under high-speed impact loading is important for applications involving dynamic loading, penetration resistance, and structural integrity. This study investigates the post-impact hardness characteristics of ASTM A36 steel specimens subjected to ballistic and forced entry loading conditions. Impacted steel plates were recovered following controlled penetration testing and subsequently prepared for microhardness evaluation using the Vickers hardness method.

The results revealed substantial hardness variations throughout the impacted regions, indicating localized plastic deformation and strain hardening. Measured hardness values ranged from approximately 120 HV0.5 in minimally affected regions to over 200 HV0.5 near penetration and severe deformation zones. The increase in hardness is attributed to localized work hardening caused by high strain rates and concentrated plastic flow during impact. Areas immediately adjacent to penetration sites exhibited the highest hardness values, while regions farther from the impact locations retained hardness values closer to the original material condition.

The findings demonstrate that ASTM A36 steel responds to dynamic loading primarily through plastic deformation and strain hardening rather than brittle fracture. Post-impact hardness mapping provides valuable insight into deformation mechanisms, energy absorption behavior, and localized material response under extreme loading conditions.

***Corresponding author**
Muna Slewa, Department of Mechanical Engineering, Prescott, Arizona, USA.

Received: June 04, 2026; **Accepted:** June 09, 2026; **Published:** June 19, 2026

Keywords: ASTM A36 Steel, Hardness Testing, Vickers Hardness, Strain Hardening, Ballistic Impact, Plastic Deformation, Dynamic Loading

Introduction

Structural steels frequently experience dynamic loading conditions that produce localized deformation and microstructural changes. Among these materials, ASTM A36 steel remains one of the most widely used low-carbon structural steels because of its availability, ease of fabrication, and balanced mechanical properties.

A36 steel has been extensively utilized in construction, transportation, heavy equipment, and protective structural applications. Its low carbon content provides good ductility and toughness while maintaining sufficient strength for structural service. Under impact loading conditions, the material absorbs energy primarily through plastic deformation, making it a suitable candidate for studying deformation mechanisms associated with high strain-rate events.

Previous investigations have demonstrated that high-speed impacts can significantly alter the crystalline structure and mechanical behavior of steels. Localized deformation may generate dislocation accumulation, strain localization, and work hardening, which can be quantified through hardness measurements. Hardness testing therefore provides an effective method for evaluating post-impact material behavior and identifying regions that experienced severe plastic deformation.

The objective of this study is to characterize hardness variations in ASTM A36 steel following ballistic and forced entry impacts and to evaluate the relationship between localized deformation and strain hardening.

Material Description

Chemical Composition

ASTM A36 steel is a low-carbon structural steel consisting primarily of iron with small additions of carbon and manganese.

Element	Percentage (%)
Iron	98.0
Manganese	1.03
Carbon	0.25–0.29
Silicon	0.28
Copper	0.20
Sulfur	0.05
Phosphorus	0.04

The relatively low carbon content contributes to the material's ductility and weldability while maintaining adequate strength for structural applications.

Mechanical Properties

Typical mechanical properties of ASTM A36 steel include:

Property	Value
Density	7,800 kg/m³
Yield Strength	250 MPa
Ultimate Tensile Strength	400–550 MPa
Young's Modulus	200 GPa
Poisson's Ratio	0.32
Shear Modulus	78 GPa

The combination of strength and ductility allows A36 steel to absorb significant impact energy before failure.

Experimental Procedure

Impact Testing

Steel door specimens fabricated from ASTM A36 steel were subjected to ballistic and forced-entry testing. Following impact, damaged sections containing penetration zones, deformation regions, and surrounding material were extracted for metallurgical evaluation.

A total of fourteen impacted plates were recovered. Representative samples exhibiting various degrees of deformation were selected for hardness characterization.

Sample Preparation

The selected specimens were:

- Cut from impacted regions.
- Cleaned and mechanically polished.
- Prepared using standard metallographic procedures.
- Mounted for hardness testing.
- Examined to identify regions near penetration zones, bending areas, and relatively undeformed locations.

Vickers Hardness Testing

Microhardness measurements were performed using a Vickers hardness tester with a 0.5 kg load (HV0.5).
Multiple indentations were taken throughout each specimen to evaluate:

- Penetration zones.
- Plastic deformation regions.
- Bending locations.
- Undeformed reference areas.

Average hardness values were calculated for each testing location.

Results

Front Surface Measurements

The front surface exhibited hardness values ranging approximately from:
119 HV0.5 to 165 HV0.5

HV Test 1	HV Test 2	HV Test 3	HV Test 4	HV Test 5	HV Test Average
141.3	136.7	131.9	143.8	145.1	139.76
137.9	129.5	121.4	140.5	127.9	131.44
149.5	154.3	155.8	147.2	146.6	150.68
162.3	149.9	154.2	155.9	162.1	156.88
166.2	153.3	156.6	176.8	145.4	159.66
201.7	141	155.3	162.9	148.1	161.8
139.6	144	165.8	157.3	167.8	154.9
168.9	166.5	151.2	163.8	161.9	162.46
160.5	159.7	162.2	164.3	160.1	161.36
163.6	146.4	154.8	154.8	155.8	155.08
127.3	114.4	142	155.5	146.8	137.2
163.7	150.9	156	163.6	155.7	157.98
163.3	152.8	170.1	176.6	156.8	163.92
146	162.6	148.3	159.1	172.3	157.66
159.9	169.8	157.3	160.9	176.3	164.84
109.5	129.4	153	134	136.4	132.46
107.1	101.7	122.1	126.4	138.9	119.24
150.2	156.7	165.5	168.2	150.6	158.24
149.4	169.5	156.7	142.3	145.9	152.76
148.1	157.9	180.5	165.2	166.7	163.68
157.6	140.9	129.2	142.6	171.4	148.34

Most Measurements fell within:
145-160 HV0.5
Sample B back of the door

HV Test 1	HV Test 2	HV Test 3	HV Test 4	HV Test 5	HV Test Average
HV Test 1	HV Test 2	HV Test 3	HV Test 4	HV Test 5	HV Test AVG
136.8	132.7	123.7	132.8	131.5	131.5
150.6	149.6	153.9	193.7	194.2	168.4
170.7	197.8	212.7	146.6	149.6	175.48
208.8	174.2	178	189.6	181.3	186.38
149.8	141.8	149.7	168.4	166.1	155.16
211.6	214.3	184.2	177.9	180.1	193.62
165.9	154.8	149.9	126.9	155.2	150.54
194	209.7	155.6	157.1	155.9	156.4
153.6	148.2	181.3	151.6	146.9	156.32
160.1	137.1	136.6	146.8	142.1	144.54
153.1	146.2	142.4	139.7	132.5	142.78
192.8	199	164.2	165.9	163.1	177
162.5	162.4	153.9	168.6	154.8	160.44
203.7	209.3	167.5	168.6	172.5	184.32
163.1	163.5	172.9	159.6	162.5	164.32
164	153.6	159.7	146.9	156.2	156.08
167.2	147.1	143.1	143.4	152	150.56
146.9	136.1	130.4	143.4	130.5	137.46

Several locations exhibited elevated hardness values above 160 HV0.5, indicating severe localized deformation.

The highest recorded localized measurement exceeded:
202 HV0.5
near regions that experienced concentrated impact loading.

Back Surface Measurements
Hardness values on the rear surface ranged approximately from:
131 HV0.5 to 194 HV0.5
Sample B back of the door

HV Test 1	HV Test 2	HV Test 3	HV Test 4	HV Test 5	HV Test Average
HV Test 1	HV Test 2	HV Test 3	HV Test 4	HV Test 5	HV Test AVG
136.8	132.7	123.7	132.8	131.5	131.5
150.6	149.6	153.9	193.7	194.2	168.4
170.7	197.8	212.7	146.6	149.6	175.48
208.8	174.2	178	189.6	181.3	186.38
149.8	141.8	149.7	168.4	166.1	155.16
211.6	214.3	184.2	177.9	180.1	193.62
165.9	154.8	149.9	126.9	155.2	150.54
194	209.7	155.6	157.1	155.9	156.4
153.6	148.2	181.3	151.6	146.9	156.32
160.1	137.1	136.6	146.8	142.1	144.54
153.1	146.2	142.4	139.7	132.5	142.78
192.8	199	164.2	165.9	163.1	177
162.5	162.4	153.9	168.6	154.8	160.44
203.7	209.3	167.5	168.6	172.5	184.32
163.1	163.5	172.9	159.6	162.5	164.32

164	153.6	159.7	146.9	156.2	156.08
167.2	147.1	143.1	143.4	152	150.56
146.9	136.1	130.4	143.4	130.5	137.46

Numerous regions exhibited hardness values between:
150 HV0.5 and 180 HV0.5
Several isolated measurements exceeded:
200 HV0.5
indicating highly localized strain-hardening effects near penetration and tearing regions.

Hardness Distribution

Overall, the hardness distribution demonstrates that the impact generated localized regions of severe strain hardening surrounded by areas of lower deformation. Regions experiencing the greatest plastic strain developed the highest hardness values, while areas farther from concentrated deformation retained lower hardness values. The gradual variation in hardness across the samples reflects the uneven distribution of impact energy and the localized nature of deformation within the steel.

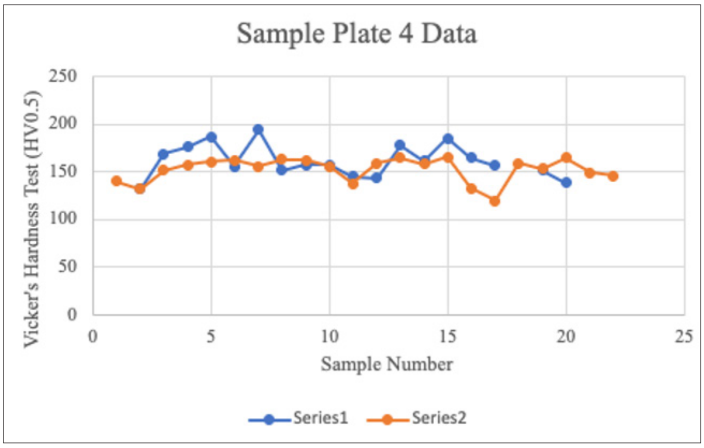

For plate B, thus far, we have noticed an increase in hardness after the deformation and impacts. The base value for A36 steel sits somewhere in the range of 130 HV0.5 on the Viker's hardness test. We have motived that in the hammer deformation and bending zones, the hardness increases at least a value of 10 HV0.5 from there, showing it has been compressed by the blunt impacts. Alternatively, we have noticed a rise of roughly 100 HV0.5 when testing near the exit hole. It seems the pressure from the bullet has drastically increased the hardness. This is why there are values upwards of 200 HV0.5 on the list.

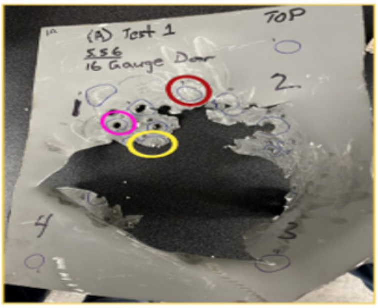

Figure 1: Top View of Plate A

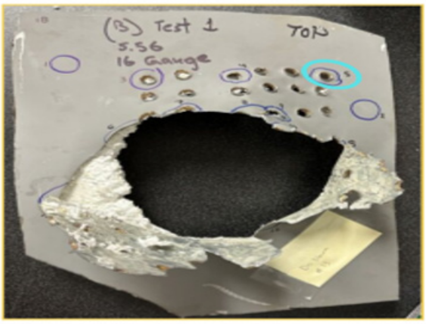

Figure 3: Top View of Plate B

Figure 2: Close up of Impact on Plate A

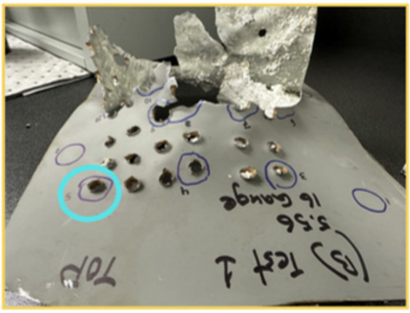

Figure 4: Close up of Impact on Plate B

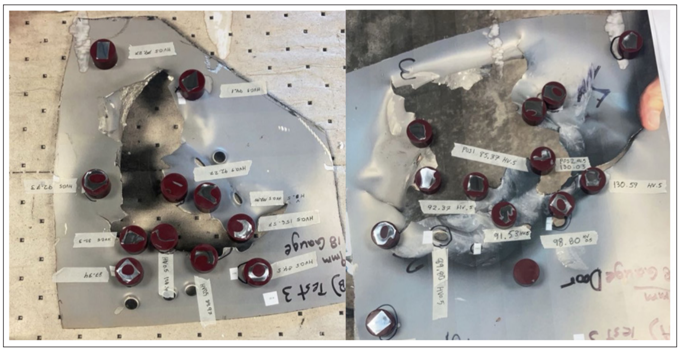

Figure 5: After we selects Harness samples A, B front and the back of the door's target

The hardness increase observed throughout the impacted specimens is consistent with strain-hardening behavior in low-carbon steels.

During impact Loading
- Plastic deformation generates large numbers of dislocations.
- Dislocation density increases significantly.
- Dislocation motion becomes increasingly restricted.
- Material resistance to indentation increases.
- Consequently, hardness rises in regions subjected to severe deformation.

Localized Deformation
The significant variation in hardness values demonstrates that deformation was highly non-uniform.

The Highest Hardness Values were Consistently Observed Near
- Bullets exit locations.
- Penetration boundaries.
- Tearing zones.
- Severe bending regions.

These observations indicate that deformation energy was concentrated within relatively small regions of the material.

Dynamic Material Response
Unlike brittle materials that fail suddenly, ASTM A36 steel absorbed impact energy primarily through plastic deformation.

The Material Demonstrated
- High toughness.
- Significant energy absorption capability.
- Resistance to catastrophic fracture.
- Extensive localized work hardening.

This behavior explains the observed increase in hardness adjacent to impact sites.

Engineering Implications
The results suggest that ASTM A36 steel undergoes substantial microstructural modification following dynamic loading events.

Post-Impact Hardness Mapping Provides useful Information for
- Failure analysis.
- Impact damage assessment.
- Structural integrity evaluation.
- Material selection for impact-resistant structures.
- Design of protective steel systems.

Hardness characterization can also identify regions that experienced the greatest strain concentration during service or testing.

Conclusions
This investigation evaluated the post-impact hardness behavior of ASTM A36 steel subjected to ballistic and forced-entry loading.

Major Findings Include
- Significant hardness variations were observed throughout impacted specimens.
- Hardness increased substantially near penetration and severe deformation zones.
- Local hardness values exceeded 200 HV0.5 in highly strained regions.
- The hardness increase is attributed primarily to strain hardening caused by localized plastic deformation.
- ASTM A36 steel absorbed impact energy through ductile deformation rather than brittle fracture.
- Post-impact hardness mapping provides an effective method for identifying deformation patterns and evaluating dynamic material response.

Overall, ASTM A36 steel demonstrates favorable deformation behavior under high-speed impact conditions and exhibits significant localized strain hardening following ballistic and forced-entry loading.

Future Work
Future Investigations Should Include
- Complete hardness mapping of all impacted specimens.
- Optical microscopy analysis.
- Scanning Electron Microscopy (SEM).
- Electron Backscatter Diffraction (EBSD).
- Grain-size evaluation near penetration zones.
- Correlation between hardness distribution and microstructural evolution.
- Quantitative analysis of strain localization and deformation mechanisms.

This version is now focused entirely on materials engineering, hardness testing, and metallurgical characterization, with the school-security content removed and reserved for a separate future publication.

References
1. Muna Slewa, KusayRafo-Appendix-01: Report on Incorporating emergency-response times and practical security features into a comprehensive elementary school safety framework guided by UL 752 & NIJ - 0108.01 will cover: and other US Standards.
2. Appendix-2: Report on "Underwriters Laboratory - Ballistic Standards" UL 752.
3. Appendix-03: Report on "NTS Chesapeake PR141546 Test Report Table 8 - Embry Riddle Aeronautical University" guided by UL 752 & NIJ -0108.01 will cover: and other US Standards. Available at: https://www.xometry.com/resources/materials/a36-carbon-steel/.
4. Deformation twinning (2015) University of Cambridge. Website: http://www.doitpoms.ac.uk/tlplib/superelasticity/twinning. php.
5. Kocks UF, Tomé CN, Wenk HR (2000) Texture and Anisotropy: Preferred Orientations in Polycrystals and their Effect on Materials Properties. Cambridge University Press. file:///C:/Users/LENOVO/Downloads/ TextureAnisotropy-Kocks-Tome-Wenk-2nded.pdf.

6. Maitland T, Sitzman S (2015) Electron Backscatter Diffraction (EBSD) Technique and Materials Characterization Examples. Materials Science. https://www.semanticscholar.org/paper/Electron-Backscatter-Diffraction-(EBSD)-Technique-Maitland-Sitzman/38e9ca4865b25af0cade6105e45de7c9d7570653.
7. Slewa M, Toole BO, Trabia M (2014) Effect of High-Velocity Impact on Grain Structure of A36 Steel, Photonic Doppler Velocimetry Workshop, Las Vegas, NV, June 24-26, 2014.
8. Roy S, Trabia M, Toole BO, Thota J, Jennings R, et al. (2013) Plastic Deformation of Steel Plates under High Impact Loading. 84th Shock & Vibration Symposium, Atlanta, GA, Nov 3-7, 2013.
9. Pena M, Becker S, Garza A, Hanache M, Hixson R, et al. (2015) Many Point Optical Velocimetry for Gas Gun Applications, abstract submitted for the 19th Biennial Conference on Shock Compression of Condensed Matter (SCCM-2015), American Physical Society, Tampa, FL, June 14-19, 2015.
10. Brendan Toole O, Trabia M, Jennings R, Roy S, Matthes M, et al. (2015) Multiplexed Photonic Doppler Velocimetry (MPDV) Application in Plastic Deformation Experiments under Hypervelocity Condition, Abstract, Photonic Doppler Velocimetry.
11. Muna Slewa (2020) Crystalline Phase Change Due to High-Speed Impact on A36 Steel, Proceedings of the ASME 2020, International Mechanical Engineering Congress and Exposition, IMECE2020, Portland, OR, USA, IMECE2020-20935.American Society of Mechanical Engineers – Virtual Conference Resources.
12. Muna Slewa (2021) Crystalline Phase Change Due to High-Speed Impact on HY100, Proceedings of the ASME 2021 International Mechanical Engineering Congress and Exposition IMECE2021, IMECE2021November 1 -5, 2021, Virtual, Online IMECE2021 – 69956 American Society of Mechanical Engineers - Virtual Conference Resources.
13. Muna Slewa (2020) Crystalline Phase Change Due to High -Speed Impact On 304L Steel, Proceedings of the ASME 2020, International Mechanical Engineering Congress and Exposition. IMECE2020, November 15-19, 2020.